

# Genetic Approach for the Determination of Object Parameters from X Ray Projections

Tayfun Günel, Sedef Kent

*İstanbul Technical University*

*Electrical & Electronics Engineering Faculty*

*Electronics and Communication Engineering Department*

*80626 Maslak, İstanbul-TURKEY*

## Abstract

*In this study, a new method is presented, based on genetic algorithms for determining object parameters such as radii and/or attenuation coefficients with some assumptions and estimating a cross-sectional image of an object from its projections obtained by X ray illumination. After it was tested for projections degraded by different random noise levels, it was observed that the genetic and fuzzy genetic algorithms improved the signal to noise ratio of the projections. The fuzzy genetic algorithm gave better results than the genetic algorithm.*

## 1. Introduction

Image reconstruction from projections developed for X ray computerized tomography is a well-known image processing technique [1]-[3]. Radon [4] established the mathematical foundations of tomography in 1917. This technique is now extensively used in many scientific, industrial and medical areas [5]. In order to reconstruct a cross-sectional image from the line integral data, a lot of algorithms exist [6]. The convolution back-projection method has great computational complexity [1],[3]. The tomographic methods based on the Fourier-Slice Theorem [7] require one dimensional (1D) Fourier transformations of the projections of the object, interpolations in the Fourier domain to estimate the 2D Fourier transformation of the object from the projections, 2D inverse Fourier transformation and application of some filtering functions in both space and frequency domains.

In this study, cross-sectional images of two different objects were estimated using genetic and fuzzy genetic optimization algorithms with some assumptions.

## 2. Projections and Noise

A shadowgram obtained by illuminating an object with penetrating radiation is known as projection. The aim of image reconstruction is to obtain an image of a cross-section of the object from these projections. This imaging technique is called transmission tomography because the transmission characteristics of the object are being imaged. The resolution is lost along the path of the X rays while obtaining the projections.

Computed tomography restores this resolution by using information from multiple projections. Therefore, image reconstruction from projections can be considered a special case of image restoration.

X rays travel in straight lines, and therefore the projection data is the measure of the line integral of some object parameters along straight lines such as attenuation coefficient. Let  $\alpha(x, y)$  denote the attenuation coefficient of the object at a point  $(x, y)$  in a slice at some fixed value of the  $z$  axis. Assuming the illumination consists of an infinitely thin parallel beam of X rays, the intensity of the detected beam is given by [1]

$$I = I_0 \exp \left[ - \int_L \alpha(x, y) du \right] \tag{1}$$

where  $I_0$  is the intensity of the incident beam,  $L$  is the path of the ray, and  $u$  is the distance along  $L$  (Figure 1). Defining the observed signal as follows

$$p = \ln(I_0/I) \tag{2}$$

the linear transformation is obtained

$$p = p(s, \theta) = \int_L \alpha(x, y) du \quad -\infty < s < \infty, \quad 0 \leq \theta < \pi \tag{3}$$

where  $(s, \theta)$  represent the coordinates relative to the object.  $L$  is the line whose normal through the origin makes angle  $\theta$  with the positive  $x$ -axis.

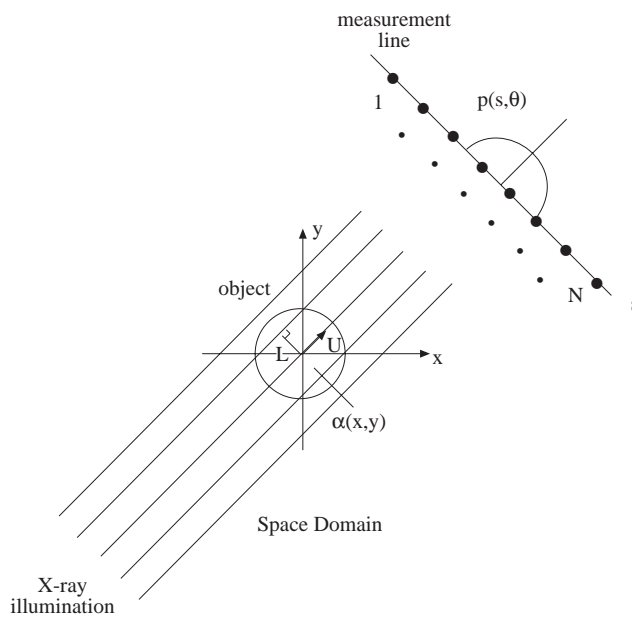


**Figure 1.** X ray illumination geometry

The projection data for an ellipse,  $p(s, \theta)$ , can be simulated using the following equation [3]:

$$p(s, \theta) = \begin{cases} \frac{2\alpha AB \sqrt{a^2(\theta) - s^2}}{a^2(\theta)} & |s| < a(\theta) \\ 0, & \text{otherwise} \end{cases} \tag{4}$$

where

$$a^2(\theta) = A^2 \cos^2(\theta) + B^2 \sin^2(\theta)$$

and  $A$  and  $B$  are the radii on the major and minor axis of an ellipse respectively,  $\alpha$  is the attenuation coefficient,  $\theta$  is the projection angle. Then, the projection function for a complex object can be calculated using the superposition and rotation properties.

The variation of the attenuation coefficient with X ray energy, artifacts and noise in the reconstruction can be cause of inaccurate characterization of objects. Noise in X ray systems has been extensively investigated in the literature [8]. The model of an image degraded by additive random noise  $u(n_1, n_2)$  is given as in [9]

$$g(n_1, n_2) = 0(n_1, n_2) + u(n_1, n_2) \quad (5)$$

where  $0(n_1, n_2)$  is the original image.

The signal to noise ratio, SNR, is defined as follows

$$SNR = 10 \log_{10} \frac{Var[0(n_1, n_2)]}{Var[u(n_1, n_2)]} \quad (6)$$

where  $Var[\cdot]$  represents the variance. The normalized mean square error (NMSE) between the original image  $0(n_1, n_2)$  and the processed image  $p(n_1, n_2)$  is defined by

$$NMSE[0(n_1, n_2), p(n_1, n_2)] = 100 \frac{Var[0(n_1, n_2) - p(n_1, n_2)]}{Var[0(n_1, n_2)]} \% \quad (7)$$

The measure NMSE  $[0(n_1, n_2), g(n_1, n_2)]$  is similarly defined [9]. The SNR improvement because of processing is defined by

$$SNR \text{ improvement} = 10 \log_{10} \frac{NMSE[0(n_1, n_2), g(n_1, n_2)]}{NMSE[0(n_1, n_2), p(n_1, n_2)]} dB \quad (8)$$

### 3. Genetic and Fuzzy Genetic Algorithms

Genetic algorithms (GAs) are known as global optimization algorithms based on evolution and genetic recombination in nature [10]. Although GA has few applications in signal processing, its potential use in signal processing is high [11]. Traditional optimization techniques use gradients and/or random searches. Gradient calculations are not used in random search methods, but gradient methods require gradient calculations. Both of them have the drawback of finding local minima instead of the global minimum. The best known global optimization techniques are based on guided random searches, such as simulated annealing [12]. The disadvantage of the simulated annealing method is that the results are very sensitive to the cooling schedule and optimization parameters, such as the initial value of temperature. Genetic algorithms that do not use any gradient calculations effectively search design space to find the 'global' minimum. A binary encoding of the parameter of the cost function to be minimized is referred to as a gene. A set of genes forms a chromosome undergoing reproduction, crossover, and mutation processes. The cost function is evaluated for each chromosome. Then, they are ranked from the lowest to the highest cost function value. Unacceptable chromosomes are eliminated after the ranking. Next, the crossover operation pairing them at a random crossover point is performed. The mutation process preventing the system from settling into local minima changes a small percentage of the bits in the chromosomes from 0 to 1 or visa versa. Although genetic algorithms are considered to be the best approach while the number of unknown parameters increases [13], it has been reported that fuzzy genetic algorithms tend to be more efficient and more suitable for some applications [14]. It is possible to fuzzify genetic algorithms by extending their gene pool to the whole unit interval  $[0 \ 1]$ . While chromosomes are coded by binary numbers in classical genetic algorithms, chromosomes in fuzzy genetic algorithms (FGAs) are represented by the numbers in  $[0 \ 1]$  as

stated in [14]. In order to apply genetic and fuzzy genetic algorithms to our problem, we simulated the projections of multilayered elliptical objects. We formed the error function as follows:

$$Error = \frac{\sqrt{\sum_{i=1}^N (P_i^m - P_i^c)^2}}{\sqrt{\sum_{i=1}^N (P_i^m)^2}} \quad (9)$$

where  $P_i^m$  is the measured or simulated projection,  $P_i^c$  is the computed projection using Eq. (4) for each chromosome consisting of unknown parameters, and  $N$  is the total number of measurement or simulation points. Using genetic and fuzzy genetic algorithms, Eq. (9) is minimized and unknown parameters are determined. This process for GA and FGA is presented in Figure 2.

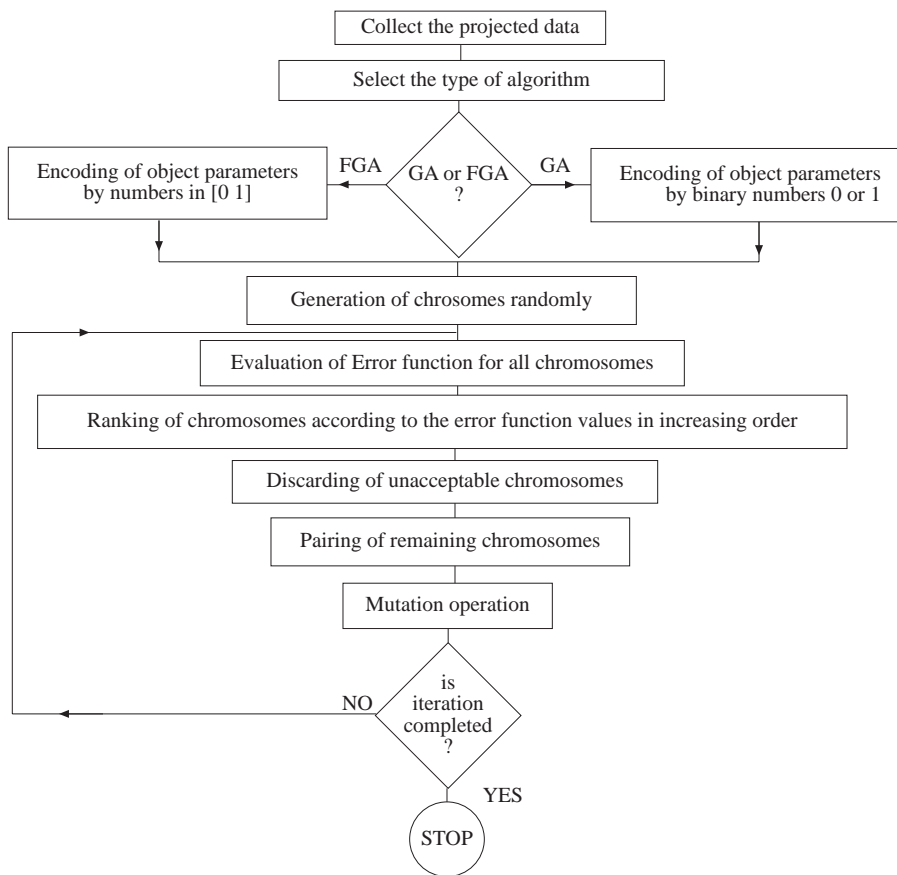


Figure 2. Flow chart of the GA and FGA approaches

## 4. Numerical Results

As a first example, a two layered circular concentric cylindrical object as shown in Figure 3 was selected. The outer radius of this object is known or it can be determined from measured projection data. The attenuation coefficients and the radius of inner layer of the object were taken as unknown parameters for optimization.

For this aim, illuminated by X ray radiation, the projection was calculated using Eq. (4) for  $N = 32$  points along  $s$  line with the length of  $l = 10$  cm and  $d = 40$  cm apart from the center of cylinders and spaced  $\Delta x = l/N$  intervals. The first layer was selected as  $\alpha_1 = 2$  and  $A_1 = B_1 = 2$  cm. The second layer was chosen as  $\alpha_2 = 1.044$  and  $A_2 = B_2 = 4$  cm. Attenuation coefficients and the radii of the cylinder can be

estimated by using the simulated projection only in one direction because of the symmetry with respect to the cylinder axis  $z$ . For asymmetrical objects, the projections around the inhomogeneous object illuminated from different directions must be measured.

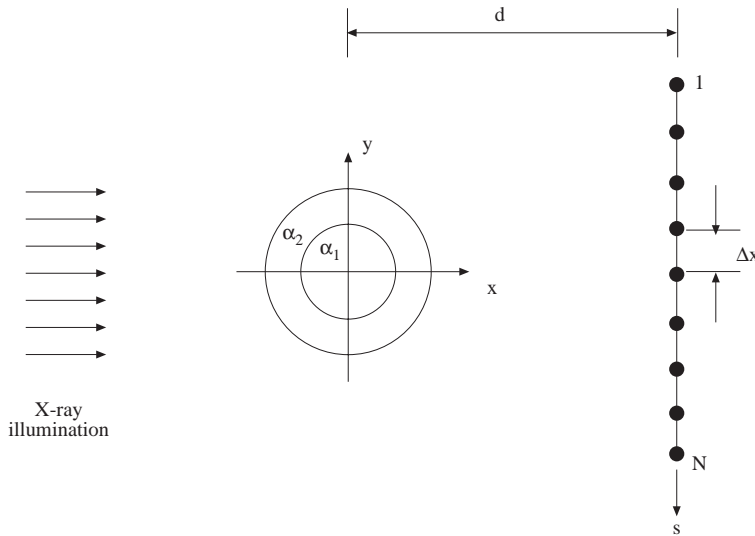


**Figure 3.** Measurement geometry of the two layered object

**Table 1.** The results for genetic and fuzzy genetic algorithms

Object parameters and computation time	Real values		Results found by Genetic Algorithm		Result found by Fuzzy Genetic Algorithm	
	1st layer	2nd layer	1st layer	2nd layer	1st layer	2nd layer
Attenuation coefficients for noise-free projections	2	1.044	2.125	1.054	1.94	1.045
Attenuation coefficients for noisy projections SNR=12.44 dB	2	1.044	2.145	1.094	2.12	1.075
Attenuation coefficients for noisy projections SNR=17.26 dB	2	1.044	2.137	1.074	2.100	1.055
Radii (cm) for noisy-free projections	2	4	2.08	4	2.02	4
Radii (cm) for noisy projections SNR=12.44 dB	2	4	2.12	4	2.09	4
Radii (cm) For noisy projections SNR=17.26 dB	2	4	2.10	4	2.07	4
Time (sec.)	-		314		296	

For the application of genetic and fuzzy genetic algorithms, the search interval for attenuation coefficients was chosen as  $0 \leq \alpha_{1,2} \leq 3$ , and the search interval for the radius of inner cylindrical object was chosen as  $0 \leq A = B \leq 4$  cm. The projection data obtained by the genetic algorithm and fuzzy genetic

algorithm were compared with the original projection data in Figure 4 and Figure 5, respectively. A similar comparison was made for projection data degraded by different noise levels in Figure 6 and Figure 7 for SNR = 12.44 dB and in Figure 8 and Figure 9 for SNR = 17.26 dB. Mean errors for both algorithms are given in Figure 10. The fuzzy genetic algorithm required fewer iterations and gave more accurate results than the genetic algorithm. The results of the genetic and fuzzy genetic algorithms are given in Table 1. Figure 11 shows the estimated image of the two-layered circular concentric cylindrical object reconstructed from the projections obtained using the fuzzy genetic algorithm.

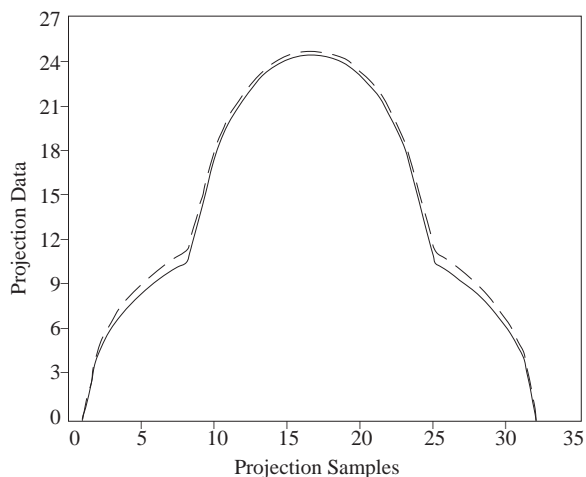


**Figure 4.** Original projection data (—), and the projection data obtained as a result of the genetic algorithm (— — —)

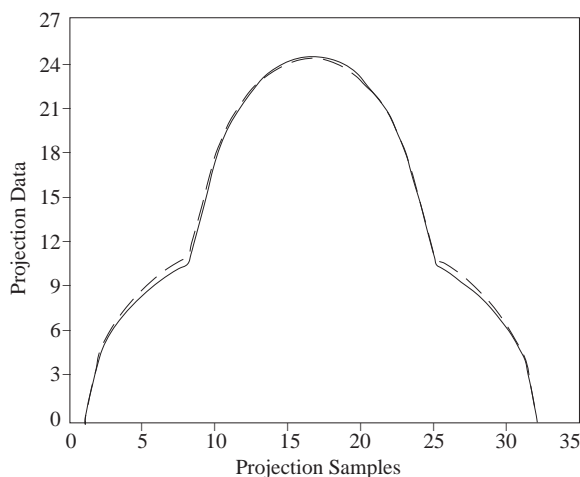


**Figure 5.** Original projection data (—), and the projection data obtained as a result of the fuzzy genetic algorithm (— — — —)

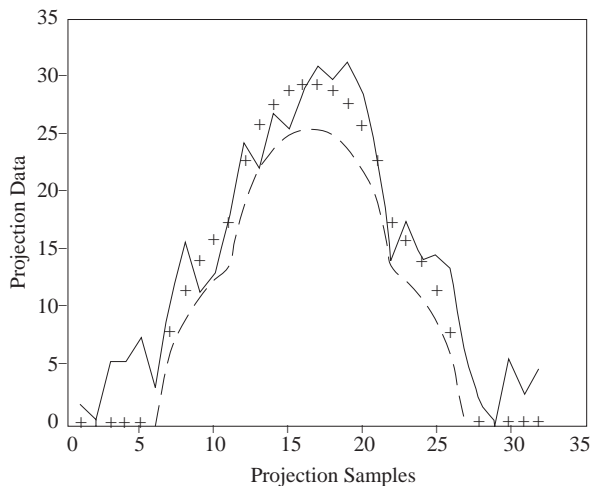


**Figure 6.** Original projection data (— — —), degraded projection data at SNR of 12.44 dB (—) and the projection data obtained as a result of the genetic algorithm with SNR improvement of 2.67 dB (++++)

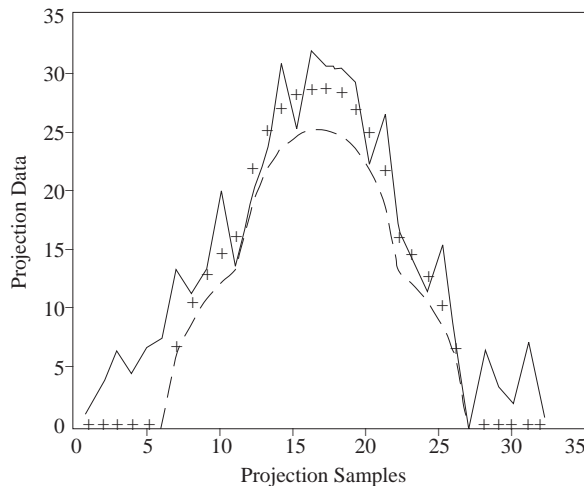


**Figure 7.** Original projection data (— — —), degraded projection data at SNR of 12.44 dB (—) and the projection data obtained as a result of the fuzzy genetic algorithm with SNR improvement of 3.6 dB (++++)

For testing GA and FGA, a head phantom identical to Shepp and Logan [2] was also chosen. Each ellipse was assigned a gray level as indicated in Table 2. By using two perpendicular projections parallel

to the major and minor axes of the phantom and applying the GA and FGA, gray levels (GL) were as given in Table 2. The reconstructed images are shown in Figure 12-(a) and Figure 12-(b) for GA and FGA, respectively. The gray levels of ellipses were selected as unknown parameters for each algorithm. The search interval for gray levels was selected as  $-1 \leq GL \leq 2$ . As seen in Table 2, the fuzzy genetic algorithm gave more accurate results than the genetic algorithm.

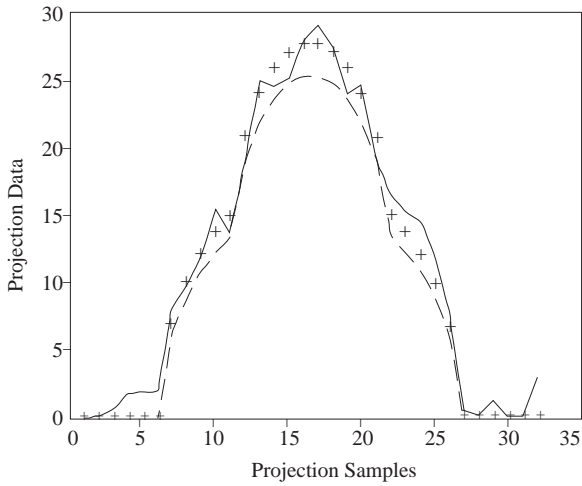


**Figure 8.** Original projection data (----), degraded projection data at SNR of 17.26 dB (—) and the projection data obtained as a result of the genetic algorithm with SNR improvement of 2.25 dB (++++)

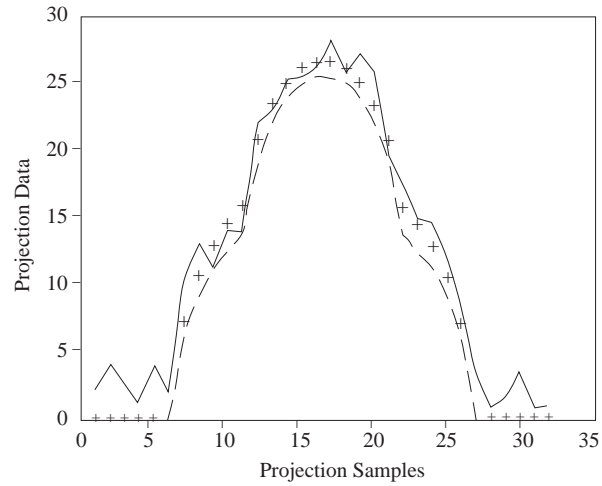


**Figure 9.** Original projection data (----), degraded projection data at SNR of 17.26 dB (—) and the projection data obtained as a result of the fuzzy genetic algorithm with SNR improvement of 3.4 dB (++++)

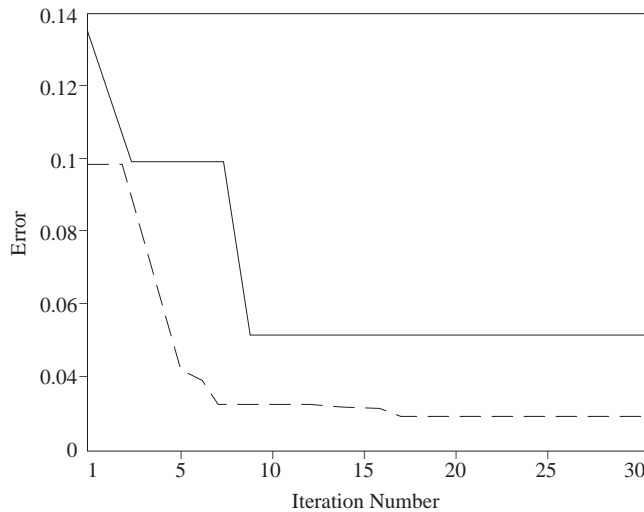


**Figure 10.** Mean errors versus iteration number (SNR = 12.44 dB and SNR = 17.26 dB). For genetic algorithm (—), for fuzzy genetic algorithm (----)

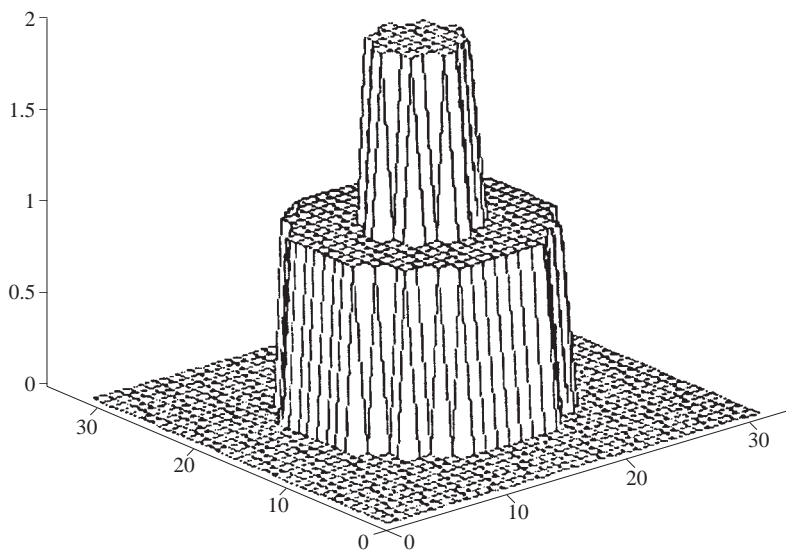


**Figure 11.** The estimated image of the two-layered circular concentric cylindrical object

**Table 2.** Parameters of shepp and logan head phantom [2] and gray levels obtained by the GA and FGA approaches

Ellipses	Center	Major Axis	Minor Axis	Inclination	Gray Level (Real values)	Gray Level (Found by GA)	Gray Level (Found by FGA)
a	0,0	0.69	0.92	0	2	1.985	1.995
b	0,-0.0184	0.6624	0.874	0	-0.98	-0.978	-0.98
c	0.22,0	0.11	0.31	-18	-0.02	-0.022	-0.021
d	-0.22,0	0.16	0.41	18	-0.02	-0.021	-0.02
e	0.035	0.21	0.25	0	0.01	0.009	0.01
f	0.01	0.046	0.046	0	0.01	0.009	0.01
g	0,-0.1	0.046	0.046	0	0.01	0.009	0.01
h	-0.08,-0.605	0.046	0.023	0	0.01	0.009	0.01
i	0,-0.605	0.023	0.023	0	0.01	0.009	0.01
j	0.06,-0.605	0.023	0.046	0	0.01	0.009	0.01

Each bit was randomly given a value in the interval [0 1] for the fuzzy genetic algorithm. Each chromosome consisted of 5 bits/parameter for both algorithms. If more bits are used, it is possible to obtain greater accuracy in spite of slow convergence. The total number of chromosomes was chosen as equal to 10 times the total number of bits in a chromosome. The bottom 50 % of them were eliminated after the ranking of the chromosomes. The remaining chromosomes were paired at randomly selected crossover points, such as the first and the third, second and fourth, etc. Mutation was performed for 1% of the chromosomes at each iteration. The algorithms were run for 30 iterations. To obtain the results, we used a PC with a Pentium 100 processor and the program codes were written in C.

## 5. Conclusion

In this study, a new method is presented, based on genetic and fuzzy genetic algorithms for determining attenuation coefficients with some assumptions and the estimation of a cross section of inhomogeneous



cylindrical objects illuminated by a X ray radiation. These algorithms were applied to two different objects. After this method was tested for projections degraded by different random noise levels it was observed that the genetic and fuzzy genetic algorithms improved the signal to noise ratio of the projections. This new approach has a global search capability and its implementation is simple. The results showed that the fuzzy genetic algorithm gave better results than the genetic algorithm.

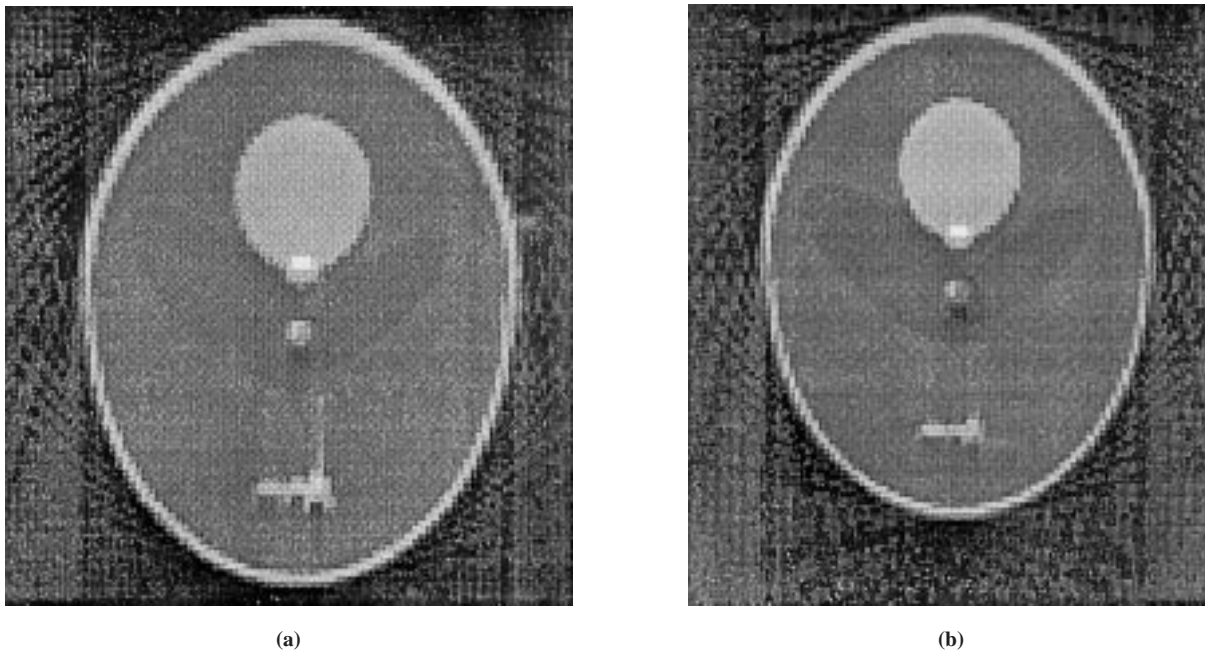


**Figure 12.** Reconstructed image of the head phantom (a) Using GA (b) Using FGA

## References

- [1] H.J. Scudder, "Introduction to computer aided tomography", *Proc. IEEE*, **6** (1978), pp.628-637.
- [2] L.A. Shepp and B.F. Logan, "The Fourier reconstruction of a head section", *IEEE Trans. On Nuclear Science*, **21** (1974), pp.21-43.
- [3] G.T. Herman, ed., *Image reconstruction from projections*, New York, Academic Press, 1980.
- [4] J. Radon, "On the determination of functions from their integrals along certain manifolds", *Ber. Saechs. Akad. Wiss. Leipzig, Mat. Physics Kl* **69** (1917), pp.262-277.
- [5] H. Lee, G. Wade, ed., *Imaging technology*, IEEE Press, New York, 1986.
- [6] A. Rosenfeld and A.C. Kak, *Digital picture processing*, II. Ed., Vol.1, New York: Academic Press, 1982.
- [7] R.M. Merseraeau and A.V. Oppenheim, "Digital reconstruction of multidimensional signals from their projections", *Proc. IEEE*, **62**, (1974), pp.1319-1338.
- [8] R.E. Alvarez, J.P. Stonestrom, "Optimal solution of computed tomographic images using experimentally measured noise properties", *Journal Computer-Assisted-Tomography*, Vol.3, (1979), pp.77-84.
- [9] J.S. Lim, *Two-dimensional Signal and Image Processing*, Prentice Hall, Inc. 1990.
- [10] J.H. Holland, "Genetic algorithms", *scientific american* (1992), pp.66-72.

- [11] K.S. Tang, K.F. Man, S.K. Wang, Q. He, "Genetic algorithms and their applications", *IEEE Signal Processing Magazine* **13** (1996), pp.22-37.
- [12] S. Kirkpatrick, C.D. Gellat, Jr., and M.P. Vecchi, "Optimization by simulated annealing", *Science* **220** (1981), pp.671-680.
- [13] R.L. Haupt, "An introduction to genetic algorithms for electromagnetics", *IEEE Antennas and Propagation Magazine* **137** (1995), pp.7-15.
- [14] G.J. Klir and B. Yuan, *Fuzzy Sets and Fuzzy Logic: Theory and Applications*, Prentice Hall, 1995.

### BOOK REVIEW

F. A. Aliev and V. B. Larin, *Optimization of Linear Control Systems: Analytical Methods and Computational Algorithms*, Gordon and Breach Science Publishers, 1988 (ISBN 90-5699-113-2)

This book on linear control systems represents an approach of two experts to  $H_2 - H_x$  techniques on the analysis and synthesis of linear control systems. Presentation of material is quite theoretical although the authors always end the theory with related algorithms. Contents of the book with respect to chapters is as follows:

Solution techniques are developed to the nonstandard LQG problem by modifying state space methods in Chapter 1. The last section deals with the problem of optimal regulator synthesis in cases where the system dynamics are described by a periodic system of difference and/or differential equations. The frequency domain methods have been investigated in Chapter 2. The approach preferred is based on Wiener-Hopf equation and minimization of the  $H_2$  norm. Chapter 3 deals with the development of computing procedures involved with the realization of algorithms in the state space approach. These algorithms are also used in Chapter 4 in developing numerical methods associated with the realization of frequency domain methods (spectral factorization and J-factorization of matrix polynomials and matrix polynomials), of optimization.

While reading this book I have noticed certain things which, I think should better be presented here. First of all, there is little or no background material in the book. On the other hand, reader is prepared to making research in the topics of  $H_2 - H_x$  techniques throughout the book though I would prefer to have some open problems suggested or hinted in a book of this caliber. As already understood the intended readers should be researchers in the  $H_2 - H_x$  fields of control (but it can not be a text book in those topics either). There are many algorithms presented but practical simulations of the algorithms and case studies are quite weak or not presented. In addition, it would be better to have more up to date references from the so-called western literature. Lastly, there are too much simple typographical errors. Probably, most of my criticizing remarks would not have been made in a second edition of this book.

In summary, this book involving the contributions and scientific tastes of two prominent researchers in the field of control theory is strongly advisable to senior graduate students and researchers in the fields of  $H_2 - H_x$  techniques on the analysis and synthesis of linear control systems.

Kemal Leblebicioğlu  
Electrical and Electronics Engineering Dept.  
Middle East Technical University  
06531, Ankara  
kleb@metu.edu.tr

## CONTENTS

<i>State of Art in Realistic Head Modeling for Electro-magnetic Source Imaging of the Human Brain</i> .....	167
N. G. GENÇER, İ. O. TANZER, M. K. ÖZDEMİR, C. E. ACAR, M. SUNGUR	
<i>Imaging Tissue Conductivity via Contactless Measurements: A Feasibility Study</i> .....	183
N. G. GENÇER, M. N. TEK	
<i>Imaging electrical current density using nuclear magnetic resonance</i> .....	201
M. EYÜBOĞLU, R. REDDY, J. S. LEIGH	
<i>Use of the magnetic field generated by the internal distribution of injected currents for Electrical Impedance Tomography (MR-EIT)</i> .....	215
Y. Z. İDER, Ö. BİRGÜL	
<i>Fdd Evaluation of the Sar Distribution in a Human Head Near a Mobile Cellular Phone</i> .....	227
S. PAKER, L. SEVGİ	
<i>Cardiac Passive Acoustic Localization: Cardiopal</i> .....	243
Y. BAHADIRLAR, H. Ö. GÜLÇÜR	
<i>Functional Radionuclide Imaging Algorithm Based On The Appended Curve Deconvolution Technique And Its Use In The Diagnosis Of Renovascular Hypertension</i> .....	261
İ. KARAGÖZ, H. AYHAN	
<i>Genetic Approach for the Determination of Object Parameters from X Ray Projections</i> .....	277
T. GÜNEL, S. KENT	
<i>BOOK REVIEW</i> .....	287